ELSEVIER

Ceramics International 32 (2006) 479–485

CERAMICS INTERNATIONAL

www.elsevier.com/locate/ceramint

Effects of Zr/Ti ratio on structural, dielectric and piezoelectric properties of Mn- and (Mn, F)-doped lead zirconate titanate ceramics

Eric Boucher [a,b,*], Benoit Guiffard [b], Laurent Lebrun [b], Daniel Guyomar [b]

[a] *Sciences des Procédés Céramiques et de Traitements de surface, UMR 6638, Faculté des Sciences et Techniques, Université de Limoges, 123 Avenue Albert Thomas, 87060 Limoges Cedex, France*

[b] *Laboratoire de Génie Electrique et Ferroélectricité, INSA de LYON, bât Gustave FERRIE, 8 rue de la physique, 69621 Villeurbanne Cedex, France*

Received 21 December 2004; received in revised form 31 January 2005; accepted 30 March 2005
Available online 25 May 2005

Abstract

The influence of the Zr/Ti ratio on the piezoelectric properties of (Mn and 1 at.% F)-doped PZT and Mn-doped PZT ceramics is investigated. Lead zirconate titanate ceramics (PZT) are prepared from chemical route based on co-precipitation of oxalates and hydroxides. Structural analysis (XRD) and measurement of electrical properties were carried out. Scanning electron microscopy is used to determine the grain size of the materials. The valency states of Mn in fluorinated PZT ceramics are studied by Electron Spin Resonance (ESR). From the experimental results, the F–O substitution increases the piezoelectric activity at the morphotropic phase boundary (MPB) and the Q_m in the rhombohedral region. In the (Mn, F)-co-doping case, the high-piezoelectric activity found at the MPB is due to an electron transfer mechanism that involved the three valency states of manganese whereas the improvement of Q_m can be explained by the valence state of manganese and the dipole defect concept.

Keywords: A. Precursors: organic; B. Microstructure-final; C. Piezoelectric properties; D. PZT

1. Introduction

Lead zirconate titanate (PZT) ceramics, with general chemical formula $PbZr_{1-x}Ti_xO_3$, are commonly used in numerous piezoelectric transducers. In these applications, PZT ceramics are used owing to their excellent dielectric and piezoelectric properties.

In practice, PZT is rarely used in a chemically pure form. The dielectric and piezoelectric properties of PZT can be modified by adding donor (inducing soft characteristics) or acceptor (hard dopant) ions to the ABO_3-type PZT perovskite structure. During the last 15 years, our Laboratory elaborated PZT ceramics doped with fluorine ion [1]. It has been demonstrated that the F–O substitution associated with lower valence cation in B-site leads to lower piezoelectric activity and/or high-mechanical quality factor. Recently, we developed a PZT co-doped with 1 at.% manganese (acceptor) and 1 at.% fluorine (donor) exhibiting high-piezoelectric and dielectric constants and quite high-mechanical quality factor at the MPB, for the 52/48 Zr/Ti ratio. (Mn, F) co-doping produces semi-hard materials with the advantages of both soft and hard materials. Eyraud et al. previously suggested that the particular behavior of (Mn, F)-co-doped PZT was due to an electron transfer mechanism between $Mn^{\alpha+}$ ions with different valency states ($\alpha = 2, 3, 4$) coexisting locally in the cationic sublattice [2]. This mechanism is established for the composition close to the morphotropic phase boundary. Thus, it is interesting to study the evolution of the piezoelectric and dielectric properties outwards the MPB.

The phase diagram of the binary system $PbZrO_3$–$PbTiO_3$ system was reported by Jaffe about 40 years ago [3]. The PZT solid solution possesses numerous phases and lattice structures, depending on Zr/Ti ratio and temperature. Above a Curie temperature (which is represented by a T_c-line),

* Corresponding author.
E-mail address: eric.boucher@unilim.fr (E. Boucher).

0272-8842/$30.00
doi:10.1016/j.ceramint.2005.03.028

these compounds exhibit a high symmetry, primitive cubic structure. Below the Curie temperature, a variety of cation shifts, octahedral tilts and deformations occur leading to a number of different ferroelectric structures. Titanium-rich compositions transform into tetragonal perovskite structures whereas the phase transformation in Zr-rich compositions is more complex. However, for $x < 90\%$, the structure is rhombohedral. In PZT solid solution, both tetragonal (T) and rhombohedral (R) phases coexist in a finite range of composition at the morphotropic phase boundary (MPB) although it is represented by a line [4]. To determine the true MPB composition range, it is imperative to synthesize PZT powders free from compositional fluctuations at the Zr/Ti site. Previous works have shown that high piezoelectric and dielectric coefficients are found at the MPB [3]. In particular, both dielectric constant and electromechanical coupling coefficient reach a maximum value.

In the present study, the $Pb_{0.89}(BaSr)_{0.11}(Zr_xTi_{1-x})_{0.99}Mn_{0.01})O_3$ and 1 at.% F-doped $Pb_{0.89}(BaSr)_{0.11}(Zr_xTi_{1-x})_{0.99}Mn_{0.01})O_3$ ceramics in the composition range $x = [0.4–0.7]$ have been prepared and characterised. The phase diagram and the MPB have been determined for these two series. The objective of this work is to study the influence of a Zr/Ti ratio on the piezoelectric properties, microstructure and crystallographic characteristics of the Mn- and (Mn, F)-doped PZT ceramics.

2. Experimental procedure

The ceramic materials are made in two steps, which basically involve synthesis of the powder and sintering of the powder into cylindrical rods and disks. The studied formulations were prepared by using a semi-wet process as described by Guiffard et al. [5]. The raw materials used are high-purity lead acetate, barium acetate, strontium acetate, manganese (II) acetate, tetra-*n*-butyl titanate ($Ti(OC_4H_9)_4$) and tetra-*n*-butyl zirconate ($Zr(OC_4H_9)_4$). The different cations were coprecipitated as oxalates and hydroxides in a aqueous solution of oxalic acid and the co-precipitation is controlled by adjusting the pH of the solution with ammonia. The sub-micrometer-sized lead fluoride powder was then added to the dried precipitate [1]. The precursor powder was then calcined for 10 h at low temperature (around 600 °C) to prevent the PbO volatilization and reheated at 800 °C for 4 h to ensure complete reaction.

The PZT powders are mixed with an appropriate amount of polyvinyl alcohol (PVA) binder and compacted into cylindrical rods at 1000 kg/cm^2, then sintered at 1230 °C for 4 h in a sealed alumina crucible with $PbZrO_3$ powder to maintain a PbO vapour pressure. Cylindrical specimens were cut and polished to a dimension of 15 mm in thickness and 6.35 mm in diameter. Finally, ceramics specimens were plated with silver and poled by a DC field of 3 kV/mm at 120 °C in silicon oil for one minute.

The dielectric and piezoelectric properties of the PZT ceramics were measured 24 h after poling. The piezoelectric coefficient d_{33} is given by a piezo-d_{33} berlincourt-meter and the dielectric constant ε_r is measured with a low-capacitance resonator (LCR) meter (HP4284A). The mechanical quality factor (Q_m) evaluation is performed, at low-driving signal, by using the resonance/anti-resonance of the admittance data provided by a network analyzer HP4194A in the frequency range 100 Hz–40 MHz. The Curie point evaluation of unpoled disk samples is based on the maximum detection of the permittivity at 1 kHz, with a temperature accuracy of ±1 °C.

X-ray diffraction analysis was performed on crushed sintered samples, in the $2\theta = 71–75°$ angular range. The diffractometer used is a X-Pert Pro MPD from Panalytical with an incident monochromator (Cu Kα1 radiation) and a real time multiple strip detector X'Celerator. The step size in the 2θ range is 0.0167° and the counting time per step is 300 s. The (3 1 0) reflection line of the X-ray diffraction patterns, which is used for phase identification, splits into two in the tetragonal structure whereas it does not split for the rhombohedral structure. The relative amount of rhombohedral (T_R) phase can be calculated using the following relation $T_R = (I_{(3\,1\,0)R})/(I_{(3\,1\,0)R} + I_{(3\,0\,1)T} + I_{(1\,0\,3)T})$ where $I_{(h\,k\,l)}$ is the intensity of the (h k l) peaks of the rhombohedral phase (R) and tetragonal phase (T). When strong overlapping of the reflection lines ($(3\,0\,1)_T$, $(3\,1\,0)_R$, $(1\,0\,3)_T$) occurred, refinement of the peaks was made with a Pseudo-Voigt profile function to estimate the peak intensities as see Fig. 1.

Microstructure of the sintered bodies, after being polished and chemically etched, was examined by scanning electron microscope (JEOL 840) and the mean grain size was determined by using the intercept method. Electron spin resonance (ESR) measurements of the ceramic powder were carried out at the X-band on a spectrometer RPE Varian E9 operating at a 9.5 GHz modulation. The ESR X-band spectra were recorded at −196 °C, and the magnetic field swept from zero to 10,000 G.

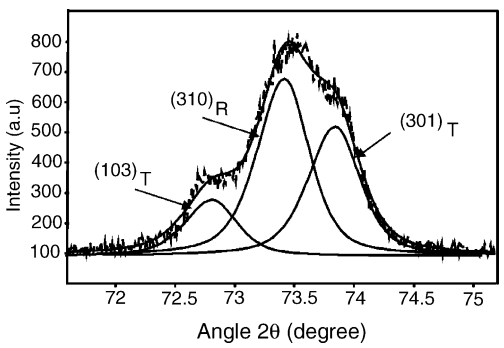

Fig. 1. Deconvolution of the profile of $(1\,0\,3)_T$, $(3\,1\,0)_R$ and $(3\,0\,1)_T$ reflection lines of biphasic PZT $Pb_{0.89}(BaSr)_{0.11}(Zr_{0.54}Ti_{0.46})_{0.99}Mn_{0.01})O_3$.

3. Experimental results

3.1. Diffractometric study

Recent studies of the PZT system revealed a narrow, monoclinic phase field in the vicinity of the MPB [6]. However, in this study, the monoclinic phase is neglected. In this case, both rhombohedral and tetragonal phases coexist for the compositions located at the morphotropic phase boundary. The amount of rhombohedral phase is calculated for nonfluorinated and fluorinated PZT ceramic versus Zr/Ti ratio at different temperatures. The schematic representations of the phase diagrams obtained for both series are shown in Fig. 2. The effect of composition on the phases can be clearly seen in this diagram. The T_c-line is the boundary between the cubic paraelectric phase and the ferroelectric phase. A MPB divides the regions of ferroelectric phase into parts: a tetragonal phase region on the Ti-rich side and a rhombohedral phase region on the Zr-rich side. The MPB is therefore not a line but a region in which tetragonal–rhombohedral phases coexist.

As for the pure PZT [1], the Curie point (T_c) increases with Ti content. Both tetragonal and rhombohedral phases coexist for x between 0.48 and 0.55 for Mn-doped PZT compositions whereas for undoped PZT, the MPB lies in the range of 0.47–0.55 [7]. The dimension of the MPB slightly decreases for (Mn, F)-co-doped PZT ($0.49 < x < 0.55$). In the MPB, there is a steep increase of relative amount of rhombohedral phase from 10 to 70% when x changes from 0.48 to 0.54.

3.2. Micrographs of SEM

Micrographs of the etched surface of Mn-doped PZT ceramic, presented Fig. 3a–c, show a uniform grain size (1–3 μm) distribution over a surface. This average grain size is nearly independent of the Zr/Ti ratio. On the contrary, in the case of (Mn, F)-co-doped PZT, the average grain size greatly increases with the amount of Ti. The average grain size increases from 2 μm to about 10 μm when the Zr/Ti ratio varies from 58/42 to 40/60, as shown in Fig. 3d–f.

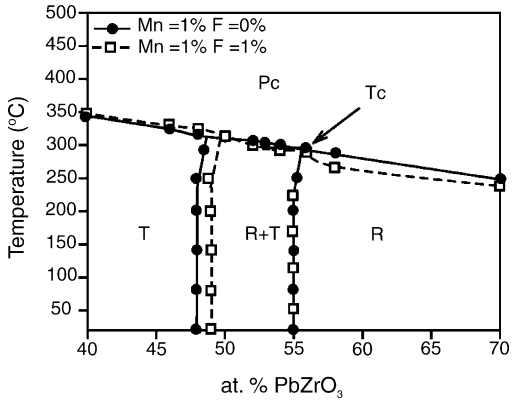

Fig. 2. Schematic phase diagram of (Mn, F)-co-doped PZT and Mn-doped PZT: Pc: paraelectric phase, F_T: ferroelectric tetragonal phase, F_R: ferroelectric rhombohedral phase.

At the MPB, for 52/48 ratio, the grain size of Mn-doped PZT is comparatively uniform, with an average value of 2 μm. The average grain size is smaller than that of pure PZT. It is well known that in acceptor-doped PZTs, the anionic sublattice contains oxygen vacancies which can act as grain growth inhibitors and prohibit the further growth of PZT grain. In the case of co-doped PZT, the introduction of fluorine makes the grain size increase. The latter are comparatively uniform, ranging from 4 to 7 μm. The PbF_2 effect on the grain growth during the sintering will be discussed in Section 4.

3.3. Dielectric and piezoelectric properties

The electrical properties, such as the dielectric, electromechanical and piezoelectric ones, are systematically evaluated depending on the Zr/Ti ratio. Figs. 4 and 5 show the variation of the d_{33} piezoelectric coefficient and mechanical quality factor (Q_m) versus the Zr/Ti ratio for (Mn and 1 at.% F)-doped PZT and Mn-doped PZT. The evolution of the coupling coefficient (k_{33}) and dielectric constant are, respectively, given in Figs. 6 and 7 for these two series. In both case of doping, the d_{33} coefficient, ε_r and coupling factor k_{33} reach a maximum value for Zr/Ti = 52/48 and their evolution versus Zr/Ti ration are very similar. Generally, high-piezoelectric activity at the MPB is attributed to the large number of thermodynamically equivalent states allows a high degree of alignment of ferroelectric dipoles. This high degree of alignment and enhanced polarizability at the MPB results in a dramatic enhancement of dielectric and piezoelectric properties approaching the MPB [3]. Recently, it has been shown that the monoclinic structure could be pictured as provided a bridge between the rhombohedral and tetragonal structures, which makes the movement of polarization easier [6]. But both interpretations do not explain the difference between the (Mn, F)-co-doped PZT and Mn-doped PZT.

On the contrary, the Q_m evolution versus Zr/Ti ratio exhibits a different trend, depending on the doping. In case of Mn doping, Q_m remains constant in both tetragonal and rhombohedral regions with higher values for tetragonal compositions. It decreases linearly through the MPB region. In case of (Mn, F)-co-doped PZT, after decreasing within the MBP, Q_m greatly increases in the rhombohedral region.

3.4. Analysis by electron spin resonance (ESR)

Previous studies have shown that the difference valency states (+2, +3, +4) of manganese coexist in the Mn-doped PZT [8–9]. For both cases of doping, the chosen manganese salt is $Mn(CH_3COO)_2{\cdot}4H_2O$, which means that the valency state of Mn is +2. However, the Mn valency state can be different in the final material, after reaction and sintering processes. When heated in air, $Mn(CH_3COO)_2{\cdot}4H_2O$ decomposed to MnO at 650 °C and an oxidation was found to occur to Mn_2O_3 at higher temperature (900 °C). The

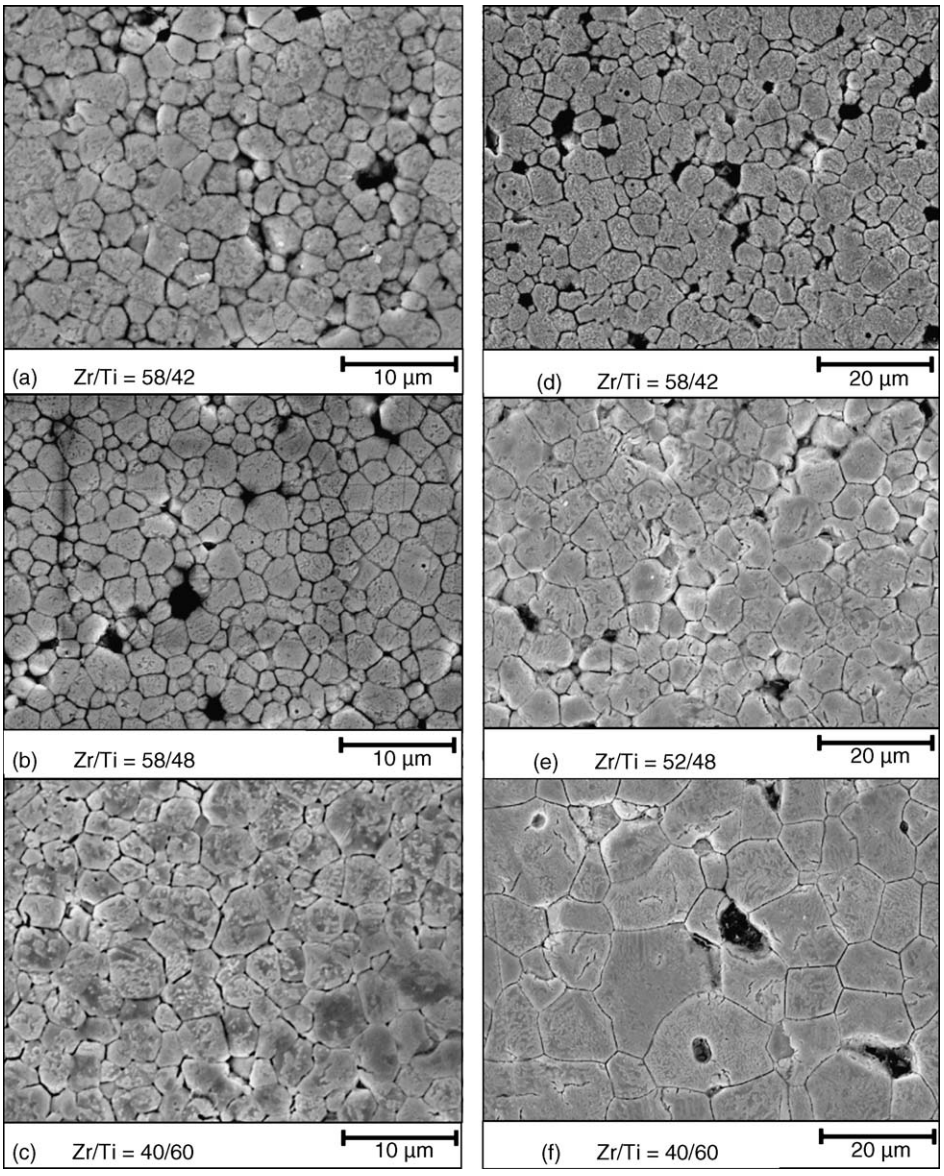

Fig. 3. Micrographs of the etched surface of Mn-doped PZT (a–c) and (Mn, F)-co-doped PZT (d–f).

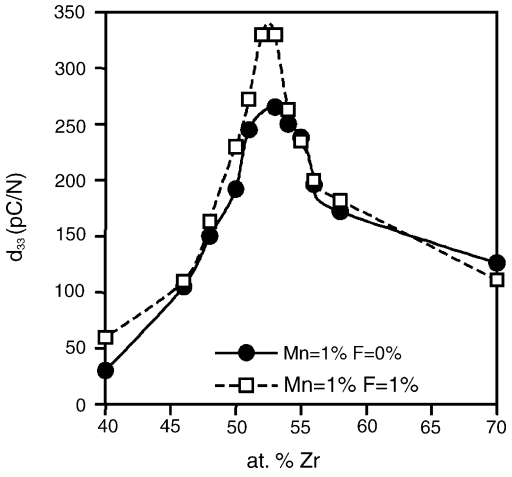

Fig. 4. d_{33} coefficient as a function of Zr content for Mn-doped PZT and (Mn, F)-co-doped PZT.

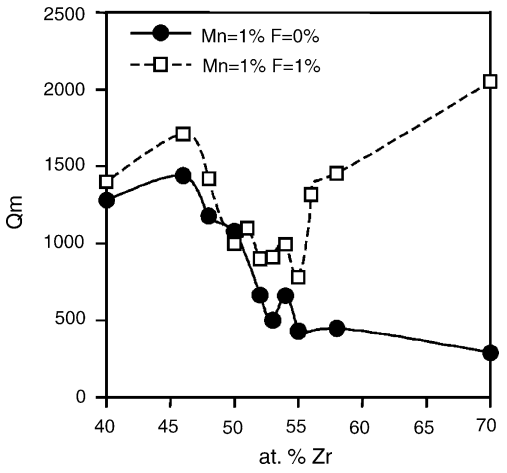

Fig. 5. Mechanical quality factor as a function of Zr content for Mn-doped PZT and (Mn, F)-co-doped PZT.

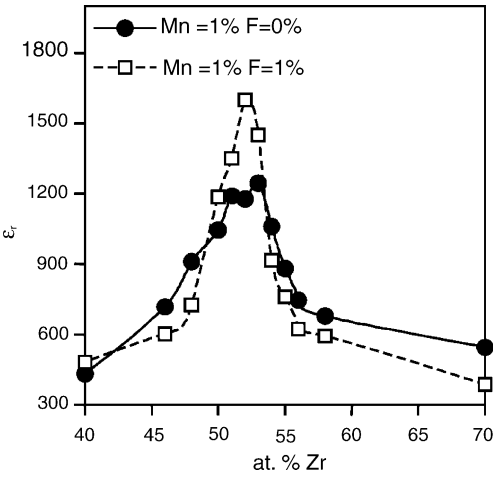

Fig. 6. Dielectric constant as a function of Zr content for Mn-doped PZT and (Mn, F)-co-doped PZT.

subsequent decomposition of Mn_2O_3 to Mn_3O_4 was found to occur in air at approximately 1000 °C. In air, Mn_3O_4 can be oxided during the cooling process. The two reactions of oxidation are given below.

$$2Mn_3O_4 + \frac{1}{2}O_2 \xrightarrow{900\,^\circ C} 3Mn_2O_3 \quad (1)$$

$$Mn_2O_3 + \frac{1}{2}O_2 \xrightarrow{600\,^\circ C} 2MnO_2 \quad (2)$$

Consequently, the oxidation state of the manganese ion can increase from +2 to +4 during the sintering process. We determined the valency states of manganese by ESR. Fig. 8 shows the ESR spectrum of Mn-doped nonfluorinated and fluorinated PZT ceramic. The existence of Mn^{2+} (peak around 3400 G) and Mn^{4+} (peak around 1500 G) was confirmed by ESR curves [8,10–11]. According to the principle of ESR, Mn^{3+} can not be detected by ESR because its has an even number of 3*d*-electrons.

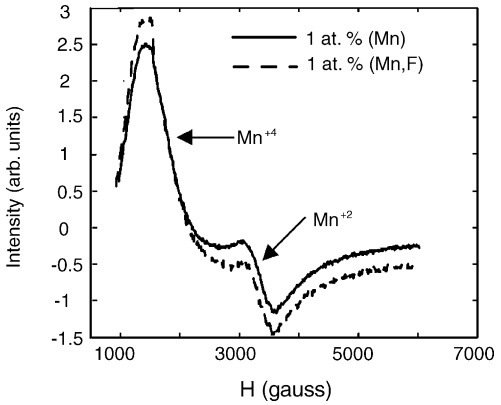

Fig. 8. ESR spectrum of Mn-doped nonfluorinated and fluorinated PZT ceramic.

The evolution of the intensity peaks versus Zr/Ti ratio is given by the ESR curves. The results obtained for (Mn, F)-co-doped PZT are given Fig. 9. The evolutions of the intensity of the Mn^{2+} and Mn^{4+} peaks are very similar. Both curves reach a minimal value at the morphotropic phase boundary. The Mn^{2+} and Mn^{4+} contents are directly proportional to the intensity of the Mn^{2+} and Mn^{4+} peaks when the samples are sintered at the same temperature. In the (Mn, F)-co-doping case, the results show that the valency states of manganese depend on the Zr/Ti ratio. We can also estimate the evolution of Mn^{3+} content versus Zr/Ti ratio. The Mn^{3+} content is defined by the following equation:

$$n_{Mn^{3+}} = n_0 - \beta I_{Mn^{4+}} - \gamma I_{Mn^{2+}} \quad \text{with} \quad n_{Mn^{2+}} = \gamma I_{Mn^{2+}} \quad \text{and} \quad n_{Mn^{4+}} = \beta I_{Mn^{4+}}$$

In this relation, n_0 is the initial content of manganese ($n_0 = 0.01$ mol), β and γ represent the proportionality coefficients and their values can be different. This result is given Fig. 10 and $n_{Mn^{3+}}$ curve reaches a maximal value at the MPB.

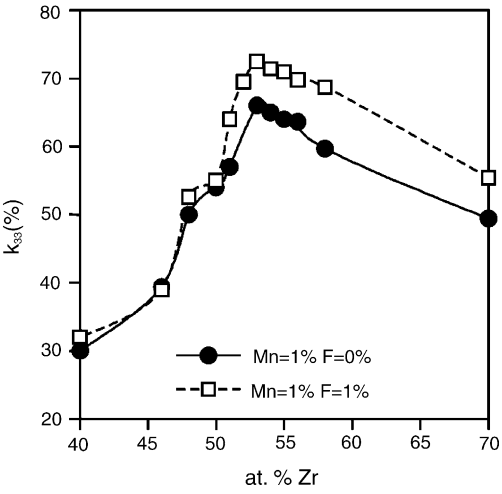

Fig. 7. Electromechanical coupling factor (k_{33}) as a function of Zr content for Mn-doped PZT and (Mn, F)-co-doped PZT.

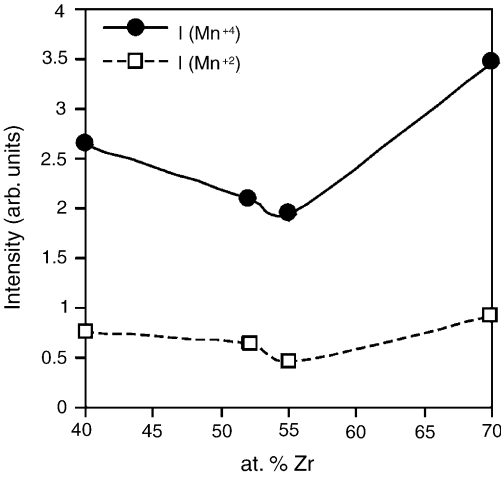

Fig. 9. Evolution of the intensity of the Mn^{2+} and Mn^{4+} peaks with the Zr content for the (Mn, F)-co-doped PZT.

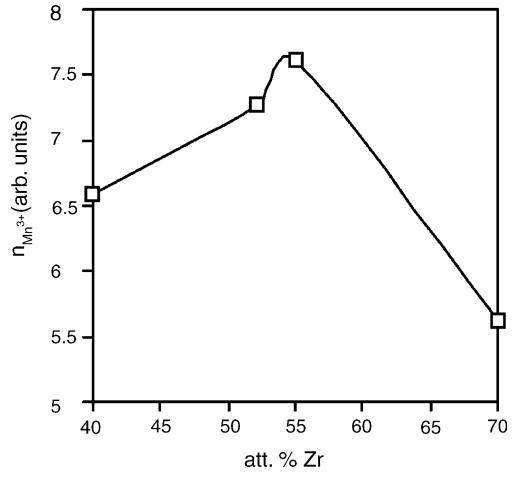

Fig. 10. Evolution of the with the Zr content for the (Mn, F)-co-doped PZT (results obtained by using the relation (1) with $\beta = \gamma = 10^{-3}$).

4. Discussion

The main effect of the fluorination is the increase of grain size versus Zr content. Ohtka et al. have shown that PbF_2 behave as a sintering aid and affect the grain growth during the sintering process [12]. Consequently, as all the formulations have been sintered at the same temperature, the grain size would be higher with F doping. It is well known that the sintering aids are used to reduce the sintering temperature and/or to increase the density of the ceramics. If PbF_2 behave as a sintering aid, the density of (Mn, F)-co-doped PZT ceramics should be higher than that of Mn-doped PZT ceramic when the samples are sintered at the same temperature. Moreover, previous studies have shown that the ceramic grain size did not change when the sintering temperature decreased [13]. Consequently, there is evidence that PbF_2 does not really behave as a sintering aid. However, there is no clear explanation why the PbF_2 effect on the grain size depends on Zr content. We have shown that several valency states (+2, +3, +4) may co-exist in (Mn, F)-doped PZT, acting as an acceptor for the valence 2+ and 3+ and as an isovalent for the valence 4+. On the same manner, it is well known that the sintering process is greatly affected by the nature of the dopant (isovalent, acceptor, donor) and by its content. For PZT doped with an acceptor such as Mn^{2+} or Mn^{3+}, the anionic sublattice contains oxygen vacancies which can act as grain growth inhibitors and prohibit the further grain growth of PZT grain. In Mn-doped PZT, the amount of oxygen vacancies is directly linked to the Mn^{2+} and Mn^{3+} content. The amount of oxygen vacancies increases with increasing Mn^{2+} and Mn^{3+} content. Consequently, if Zr content controls the Mn valence distribution and the content of each species (Mn^{2+}, Mn^{3+}, Mn^{4+}), it could control the amount of oxygen vacancies and thus the grain growth during the sintering process. The curves given Fig. 10 clearly show that the evolutions of the intensity of the Mn^{2+} and Mn^{4+} peaks on the Ti-rich side and Zr-rich side are very similar. This result suggests that the Mn^{2+} and Mn^{4+} concentration are almost equal in both cases. The increasing of the average grain size when the Zr/Ti ratio varies from 70/30 to 40/60 cannot be explained by the change of valence state of manganese. Further investigations will be necessary to clarify the mechanism, which controls the grain size of the fluorinated PZT versus Zr content.

For both Mn-doped PZT and (Mn, F)-co-doped PZT, d_{33}, ε_r and k_{33} exhibit similar trends than these one previously reported with hard or semi-hard PZT composition. High-piezoelectric activity is in particular observed at the MPB, for the 52/48 Zr/Ti ratio. The higher value of piezoelectric and dielectric coefficient obtained with (Mn, F)-doping could be explained by the larger average grain size that enhances the domain wall mobility. On the other hand, ESR spectrum has given evidence of the relative high-Mn^{4+} content and low-Mn^{2+} content in 1 at.% Mn-doped PZT [13]. In the case of (Mn, F)-co-doped PZT, the intensity of the sharp peak (3400 G) increases when fluorine is introduced in the anionic site. Consequently, this result suggests that the fluorine ion changes the valence state of manganese. A F–O substitution then takes place, and reduce the valence state of manganese. In other words, the fluorine ion may inhibit the oxidation of Mn_2O_3 during the cooling process. Unfortunately, the valency state 3+ is undetectable by ESR but the similar value of Q_m obtained for undoped PZT 52/48 ($Q_m = 600$) and for Mn-doped PZT suggests that Mn^{3+} content is certainly low and confirms low-Mn^{2+} content in these compositions. However, the different valence state of manganese between the two formulations is clearly established and could also explain the slight difference of the piezoelectric activity at the MPB. Eyraud et al. previously suggested that the high-piezoelectric activity in (Mn, F)-co-doped PZT was due to an electron transfer mechanism that involved the three valency states of Manganese [2]. The fluorine ions create (F^-, $Mn^{\alpha+}$) sites donor ($Mn^{3+} \leftrightarrow Mn^{4+} + e^-$) or acceptor ($Mn^{3+} + e^- \leftrightarrow Mn^{2+}$), which can exchange electrons. From ESR results given in Fig. 10, we can consider that this electron exchange is activated by the relative high-Mn^{3+} content at the MPB. In fact, these electron transfers are supposed to minimize space charge (ρ_p) existing at the domain walls interface due to the polarization divergences ($\rho_p = -\mathrm{div}\,\vec{P}$), making the domain wall movement easier.

Concerning Q_m evolution, Mn-doped PZT exhibits a classical behavior, with higher Q_m in the tetragonal phase and lower Q_m in the rhombohedral phase. For (Mn, F)-co-doped PZT, the behavior is clearly different especially in the rhombohedral region, where Q_m increases. In this region, the average grain size of (Mn, F)-co-doped PZT is always higher than PZT doped with manganese (Fig. 4). It is generally admitted that the increase of grain size enhances domain wall mobility and consequently decreases Q_m. There is clearly a discrepancy between this assertion and the observed experimental results. On the other hand, we can see that the mechanical quality factor remains high on the Ti-rich side (Zr/Ti = 40/60) although the average grain size is

approximately 10 times higher in the (Mn, F)-co-doped PZT than in the Mn-doped PZT. All of that suggest that the increase of Q_m cannot be explained by the change of the microstructure. Thus, two other mechanisms can control the Q_m value. The first depends on the valence state of manganese. It has been previously reported that Q_m increases with the Mn^{2+} and Mn^{3+} content [9]. It is partially confirmed by ESR analysis (Fig. 9). Indeed, the intensity of the Mn^{2+} peak exhibits a minimal value at the MPB. Consequently, the mechanical quality factor is higher on the Ti-rich side and Zr-rich side than at the MPB. The second is based on the dipole defect concept and assumes that acceptor ion/F defect dipole can stabilize the polarization within domain leading to lower domain wall mobility and consequently to an increase of Q_m. If this mechanism is valid, Mn^{2+} detected in (Mn, F)-co-doped PZT can act as an acceptor ion, which would explain the observed improvement of Q_m. It seems that this stabilization mechanism is particularly active in the rhombohedral region. As seen on Fig. 9, this high stabilization on the Zr-rich side can be explained by a higher amount of Mn^{+2}.

Further investigations concerning (Mn, F)-co-doped PZT specimens with higher fluorine concentration are necessary to clarify the fluorination mechanism versus Zr/Ti ratio.

5. Conclusion

The F–O substitution increases the piezoelectric activity and the Q_m coefficient for the PZT compositions close to the morphotropic phase boundary. The high-piezoelectric activity found at the MPB is due to an electron transfer mechanism that involved the three valency states of manganese. In case of (Mn, F)-co-doped PZT, after decreasing within the MBP, Q_m greatly increases in the rhombohedral region. The improvement of Q_m can be explained by the valence state of manganese and the dipole defect concept.

References

[1] L. Eyraud, P. Eyraud, F. Eyraud, D. Audigier, M. Boisrayon, Céramique fluorées de puissance, U.S. Patent 5,683,613 (November 1997).
[2] L. Eyraud, P. Eyraud, L. Lebrun, B. Guiffard, E. Boucher, D. Audigier, D. Guyomar, Effect of (Mn, F) co-doping on PZT characteristics under the influence of external disturbances, Ferroelectrics 266 (2001) 41–54.
[3] B. Jaffe, W.R. Cook, H. Jaffe, Piezoelectric Ceramics, Academic Press, London, 1971, 317 pp..
[4] M.R. Soares, A.M.R. Senos, P.Q. Mantas, Phase coexistence region and dielectric properties of PZT ceramics, J. Eur. Ceram. Soc. 20 (2000) 321–334.
[5] B. Guiffard, M. Troccaz, Low temperature synthesis of stochiometric and homogeneous lead zirconate titanate powder by oxalate and hydroxyde coprecipitation, Mater. Res. Bull. 33 (1998) 1759–1768.
[6] B. Noheda, J.A. Gonzalo, L.E. Cross, R. Guo, S.-E. Park, D.E. Cox, G. Shirane, Tetragonal to monoclinic phase transition in a ferroelectric perovskite: the structure of $PbZr_{0.52}Ti_{0.48}O_3$, Phys. Rev. B 61 (2000) 8687–8695.
[7] B. Guiffard, Elaboration et caractérisation de céramiques férroélectriques de type PZT fluorées, Ph.D. Thesis, INSA de Lyon, 1999 (in French).
[8] M.D. Glinchuk, I.P. Bikov, V.M. Kurliand, M. Boudys, T. Kala, K. Nejezchleb, Phys. Stat. Sol. 122 (1990) 341–346.
[9] T. Isaki, H. Haneda, A. Watanabe, Y. Uchida, J. Tanaka, S. Shirasaki, Jpn. J. Appl. Phys. 31 (1992) 3045–3047.
[10] L.X. He, C.E. Li, Effects of addition of MnO on piezoelectric properties of lead zirconate titanate, J. Mater. Sci. 35 (2000) 2477–2480.
[11] T. Kamiya, T. Suziki, T. Tsurumi, M. daimon, Effects of manganese additionon piezoelectric properties of $Pb(Zr_{0.5}Ti_{0.5})O_3$, Jpn. J. Appl. Phys. 31 (9B) (1992) 3058–3060.
[12] O. Ohtaka, R. Von Der Muhl, J. Ravez, Low temperature sintering of Pb(Zr, Ti)O_3 ceramics with the aid of oxyfluoride additive: X-ray diffraction and dielectric studies, J. Am. Ceram. Soc. 78 (3) (1995) 805–808.
[13] E. Boucher, D. Guyomar, L. Lebrun, B. Guiffard, G. Grange, Effect of (Mn, F) and (Mg, F) co-doping on dielectric and piezoelectric properties of lead zirconate titanate ceramics, J. Appl. Phys. 92 (9) (2002) 5437–5442.